

Monocationic Trihydride and Dicationic Dihydride–Dihydrogen and Bis(dihydrogen) Osmium Complexes Containing Cyclic and Acyclic Triamine Ligands: Influence of the N–Os–N Angles on the Hydrogen–Hydrogen Interactions

Miguel Baya,* Miguel A. Esteruelas,* Montserrat Oliván, and Enrique Oñate

Departamento de Química Inorgánica, Instituto de Ciencia de Materiales de Aragón, Universidad de Zaragoza, CSIC, 50009 Zaragoza, Spain

Received December 4, 2008

New monocationic trihydride and dicationic dihydride–dihydrogen and bis(dihydrogen) osmium complexes with cyclic and acyclic triamines have been prepared and characterized. The treatment of $\text{OsH}_3\text{Cl}(\text{P}^i\text{Pr}_3)_2$ (**1**) with 1,4,7-triazacyclononane (TACN) in toluene at 60 °C affords the monocationic trihydride $[\text{OsH}_3(\text{TACN})(\text{P}^i\text{Pr}_3)]\text{Cl}$ (**2**), which reacts with HBF_4 to give the dicationic dihydride–dihydrogen $[\text{OsH}_2(\text{TACN})(\eta^2\text{-H}_2)(\text{P}^i\text{Pr}_3)](\text{BF}_4)_2$ (**3**). Complex **1** also reacts with 1,4,7-triazacyclodecane (TACD) and bis(2-aminoethyl)amine (BAEA). Similarly to TACN, the reaction of **1** with TACD gives a monocationic trihydride derivative $[\text{OsH}_3(\text{TACD})(\text{P}^i\text{Pr}_3)]\text{Cl}$ (**4**), which in the presence of HBF_4 generates a dicationic dihydride–dihydrogen $[\text{OsH}_2(\text{TACD})(\eta^2\text{-H}_2)(\text{P}^i\text{Pr}_3)](\text{BF}_4)_2$ (**5**). However, the treatment of **1** with BAEA leads to the monocationic trihydride $[\text{OsH}_3(\text{BAEA})(\text{P}^i\text{Pr}_3)]\text{Cl}$ (**6**), which in the presence of HBF_4 affords the dicationic bis(dihydrogen) $[\text{Os}(\text{BAEA})(\eta^2\text{-H}_2)_2(\text{P}^i\text{Pr}_3)](\text{BF}_4)_2$ (**7**). The structures of **2–4** and **6** have been determined by X-ray diffraction analysis, and the position of the hydrogen atoms bonded to the metal center was confirmed by density functional theory calculations. The geometries of **2**, **4**, and **6** have been rationalized as pentagonal bipyramids and their behavior on the basis of the $\text{N}_{\text{meridional}}\text{–Os–N}_{\text{meridional}}$ angle of the bipyramids.

Introduction

The activation of molecular hydrogen promoted by transition-metal complexes is very sensitive to the nature of the metal, the ligands, and the charge of the complex. It is generally accepted that strongly donating ligands, 5d metals, and neutral charge favor elongation and splitting of the hydrogen–hydrogen bond to form dihydride derivatives, while electron-withdrawing ligands, 3d metals, and positive charge favor the molecular hydrogen binding to afford dihydrogen compounds.¹ On the other hand, there are poorly understood effects, under these general statements, that are made evident in the sensitivity of the hydrogen–hydrogen separation. For instance, the hydrotris(pyrazolyl)borate (Tp) ligand has a higher ability than the cyclopentadienyl (Cp)

group to stabilize nonclassical structures.² However, both ligands adopt the same facial geometry, and although there are differences between them in steric and electronic properties,³ the comparison of the $\nu(\text{CO})$ IR data for $\text{MHTp}(\text{CO})(\text{P}^i\text{Pr}_3)$ and $\text{MHCp}(\text{CO})(\text{P}^i\text{Pr}_3)$ ($\text{M} = \text{Ru},^{4,5} \text{Os}^{4,6}$) suggests that their electron-donating abilities are similar.

Osmium hydride complexes have been shown to promote carbon–carbon and carbon–heteroatom coupling reactions.⁷

- (2) For example, see: (a) Moreno, B.; Sabo-Etienne, S.; Chaudret, B.; Rodriguez-Fernandez, A.; Jalon, F.; Trofimenko, S. *J. Am. Chem. Soc.* **1994**, *116*, 2635. (b) Moreno, B.; Sabo-Etienne, S.; Chaudret, B.; Rodriguez, A.; Jalon, F.; Trofimenko, S. *J. Am. Chem. Soc.* **1995**, *117*, 7441. (c) Chan, W.-C.; Lau, C.-P.; Chen, Y.-Z.; Fang, Y.-Q.; Ng, S.-M.; Jia, G. *Organometallics* **1997**, *16*, 34. (d) Oldham, W. J., Jr.; Hinkle, A. S.; Heinekey, D. M. *J. Am. Chem. Soc.* **1997**, *119*, 11028. (e) Gelabert, R.; Moreno, M.; Lluch, J. M.; Lledós, A. *Organometallics* **1997**, *16*, 3805. (f) Chen, Y.-Z.; Chan, W. C.; Lau, C. P.; Chu, H. S.; Lee, H. L.; Jia, G. *Organometallics* **1997**, *16*, 1241. (g) Jiménez-Tenorio, M. A.; Jiménez-Tenorio, M.; Puerta, M. C.; Valerga, P. *J. Chem. Soc., Dalton Trans.* **1998**, 3601. (h) Sabo-Etienne, S.; Chaudret, B. *Coord. Chem. Rev.* **1998**, *178–180*, 381. (i) Jia, G.; Lau, C.-P. *Coord. Chem. Rev.* **1999**, *190–192*, 83. (j) Jiménez-Tenorio, M.; Palacios, M. D.; Puerta, M. C.; Valerga, P. *Organometallics* **2005**, *24*, 3088.

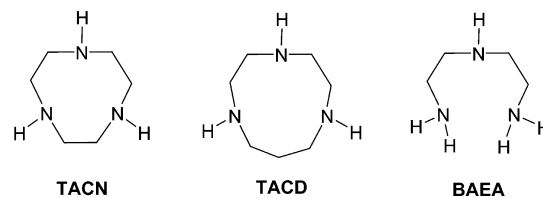
* To whom correspondence should be addressed. E-mail: miguelbayamoscu@yahoo.es (M.B.), maester@unizar.es (M.A.E.).

(1) For example, see: (a) Kubas, G. J. *Chem. Rev.* **2007**, *107*, 4152. (b) Szymczak, N. K.; Tyler, D. R. *Coord. Chem. Rev.* **2008**, *252*, 212. (c) Morris, R. H. *Coord. Chem. Rev.* **2008**, *252*, 2381.

However, it is difficult to rationalize the processes because the products from the reactions of these compounds with unsaturated organic molecules depend on the interactions within the OsH_n units,⁸ and a further understanding of them is needed. Our interest in advancing the problem's solution prompted us, recently, to carry out a systematical comparison of the structures and spectroscopic properties between the Cp complexes $\text{OsH}_3\text{Cp}(\text{P}^i\text{Pr}_3)$,⁹ $[\text{OsH}_2\text{Cp}(\eta^2\text{-H}_2)(\text{P}^i\text{Pr}_3)]\text{BF}_4^{10}$ and $[\text{OsH}_2\text{Cp}(\kappa^1\text{-OCMe}_2)(\text{P}^i\text{Pr}_3)]\text{BF}_4^{11}$ and the Tp counterparts $\text{OsH}_3\text{Tp}(\text{P}^i\text{Pr}_3)$, $[\text{OsTp}(\eta^2\text{-H}_2)(\text{P}^i\text{Pr}_3)]\text{BF}_4$, and $[\text{OsTp}(\eta^2\text{-H}_2)(\kappa^1\text{-OCMe}_2)(\text{P}^i\text{Pr}_3)]\text{BF}_4$. This study revealed that Tp avoids piano-stool structures, typical for the Cp ligand, and enforces dispositions allowing N–Os–N angles close to 90° , which favor the nonclassical interactions.¹²

A neutral analogue of the Tp and Cp ligands is 1,4,7-triazacyclononane (TACN).¹³ It also binds metals strongly to cover a trigonal face of an octahedrally coordinated

Chart 1

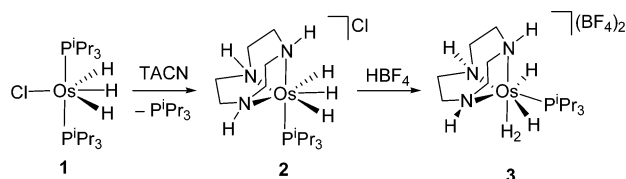


transition-metal ion, proving useful control over the remaining environment. Thus, this amine and some of its functionalized derivatives have received increased attention in recent years;¹⁴ in particular, iron¹⁵ and ruthenium¹⁶ chemistries are well established including some reports on dihydrogen complexes.¹⁷ For osmium, Taube and co-workers¹⁸ have reported some of the few known compounds.¹⁹

In our search to shed new light on how to control the interactions within OsH_n units, we have now prepared OsH_3 and OsH_4 complexes with TACN and related amines (Chart 1), such as 1,4,7-triazacyclodecane (TACD) and bis(2-aminoethyl)amine (BAEA), and compared their structures

- (3) For example, see: (a) Kitajima, N.; Tolman, W. B. *Prog. Inorg. Chem.* **1995**, *43*, 419. (b) Gemel, C.; Trimmel, G.; Slugovc, C.; Kremel, S.; Mereiter, K.; Schmidt, R.; Kirchner, K. *Organometallics* **1996**, *15*, 3998. (c) Tellers, D. M.; Bergman, R. G. *J. Am. Chem. Soc.* **2000**, *122*, 954. (d) Tellers, D. M.; Skoog, S. J.; Bergman, R. G.; Gunnoe, T. B.; Harman, W. D. *Organometallics* **2000**, *19*, 2428. (e) Rüba, E.; Simanko, W.; Mereiter, K.; Schmidt, R.; Kirchner, K. *Inorg. Chem.* **2000**, *39*, 382. (f) Tellers, D. M.; Bergman, R. G. *Organometallics* **2001**, *20*, 4819. (g) Bengali, A. A.; Mezick, B. K.; Hart, M. N.; Fereshteh, S. *Organometallics* **2003**, *22*, 5436. (h) Bergman, R. G.; Cundari, T. R.; Gillespie, A. M.; Gunnoe, T. B.; Harman, W. D.; Klinckman, T. R.; Temple, M. D.; White, D. P. *Organometallics* **2003**, *22*, 2331. (i) Brunker, T. J.; Green, J. C.; O'Hare, D. *Inorg. Chem.* **2003**, *42*, 4366. (j) Beach, N. J.; Williamson, A. E.; Spivak, G. J. *J. Organomet. Chem.* **2005**, *690*, 4640.
- (4) Bohanna, C.; Esteruelas, M. A.; Gómez, A. V.; López, A. M.; Martínez, M.-P. *Organometallics* **1997**, *16*, 4464.
- (5) Esteruelas, M. A.; Gómez, A. V.; Lahoz, F. J.; López, A. M.; Oñate, E.; Oro, L. A. *Organometallics* **1996**, *15*, 3423.
- (6) Esteruelas, M. A.; Gómez, A. V.; López, A. M.; Oro, L. A. *Organometallics* **1996**, *15*, 878.
- (7) For example, see: (a) Esteruelas, M. A.; García-Yebra, C.; Oliván, M.; Oñate, E.; Tajada, M. A. *Organometallics* **2000**, *19*, 5098. (b) Castarlenas, R.; Esteruelas, M. A.; Oñate, E. *Organometallics* **2001**, *20*, 2294. (c) Esteruelas, M. A.; Herrero, J.; López, A. M.; Oliván, M. *Organometallics* **2001**, *20*, 3202. (d) Barrio, P.; Esteruelas, M. A.; Oñate, E. *J. Am. Chem. Soc.* **2004**, *126*, 1946. (e) Barrio, P.; Esteruelas, M. A.; Oñate, E. *Organometallics* **2004**, *23*, 1340. (f) Cobo, N.; Esteruelas, M. A.; González, F.; Herrero, J.; López, A. M.; Lucio, P.; Oliván, M. *J. Catal.* **2004**, *223*, 319. (g) Bolaño, T.; Castarlenas, R.; Esteruelas, M. A.; Oñate, E. *J. Am. Chem. Soc.* **2006**, *128*, 3965. (h) Esteruelas, M. A.; Fernández-Alvarez, F. J.; Oliván, M.; Oñate, E. *J. Am. Chem. Soc.* **2006**, *128*, 4596. (i) Esteruelas, M. A.; Hernández, Y. A.; López, A. M.; Oliván, M.; Oñate, E. *Organometallics* **2007**, *26*, 2193.
- (8) For reactions with alkynes, see: (a) Castro-Rodrigo, R.; Esteruelas, M. A.; López, A. M.; Oñate, E. *Organometallics* **2008**, *27*, 3547. (b) For reactions with olefins, see Esteruelas, M. A.; García-Yebra, C.; Oliván, M.; Oñate, E. *Organometallics* **2000**, *19*, 3260. (c) For reactions with aldehydes, see: Esteruelas, M. A.; Hernández, Y. A.; López, A. M.; Oliván, M.; Rubio, L. *Organometallics* **2008**, *27*, 799, and references cited therein. (d) For reactions with aromatic and α,β -unsaturated ketones, see: Buil, M. L.; Esteruelas, M. A.; Garcés, K.; Oliván, M.; Oñate, E. *Organometallics* **2008**, *27*, 4680, and references cited therein. (e) For reactions with pyridines and quinolines, see Buil, M. L.; Esteruelas, M. A.; Garcés, K.; Oliván, M.; Oñate, E. *J. Am. Chem. Soc.* **2007**, *129*, 10998, and references cited therein.
- (9) Baya, M.; Crochet, P.; Esteruelas, M. A.; Gutiérrez-Puebla, E.; Ruiz, N. *Organometallics* **1999**, *18*, 5034.
- (10) Esteruelas, M. A.; Hernández, Y. A.; López, A. M.; Oliván, M.; Oñate, E. *Organometallics* **2005**, *24*, 5989.
- (11) Esteruelas, M. A.; Hernández, Y. A.; López, A. M.; Oñate, E. *Organometallics* **2007**, *26*, 6009.
- (12) Castro-Rodrigo, R.; Esteruelas, M. A.; López, A. M.; Oliván, M.; Oñate, E. *Organometallics* **2007**, *26*, 4498.
- (13) Chaudhuri, P.; Wieghardt, K. *Prog. Inorg. Chem.* **1987**, *35*, 329.
- (14) For example, see: (a) Köhn, R. D.; Haufe, M.; Kociuh-Köhn, G.; Filippou, A. C. *Inorg. Chem.* **1997**, *36*, 6064. (b) de Bruin, B.; Donners, J. J. M.; de Gelder, R.; Smits, J. M. M.; Gal, A. W. *Eur. J. Inorg. Chem.* **1998**, 401. (c) Baker, M. V.; North, M. R.; Skelton, B. W.; White, A. H. *Inorg. Chem.* **1999**, *38*, 4515. (d) Giesbrecht, G. R.; Cui, C.; Shafir, A.; Schmidt, J. A. R.; Arnold, J. *Organometallics* **2002**, *21*, 3841. (e) Imura, M.; Evans, D. R.; Flood, T. C. *Organometallics* **2003**, *22*, 5370. (f) Partyka, D. V.; Staples, R. J.; Holm, R. H. *Inorg. Chem.* **2003**, *42*, 7877. (g) Schmidt, J. A. R.; Giesbrecht, G. R.; Cui, C.; Arnold, J. *Chem. Commun.* **2003**, 1025. (h) Wang, D.; Zhao, C.; Phillips, D. L. *Organometallics* **2004**, *23*, 1953. (i) Braband, H.; Abram, U. *Inorg. Chem.* **2006**, *45*, 6589. (j) Ferreira, H.; Dias, A. R.; Duarte, M. T.; Ascenso, J. R.; Martins, A. M. *Inorg. Chem.* **2007**, *46*, 750. (k) Tredget, C. S.; Clot, E.; Mountford, P. *Organometallics* **2008**, *27*, 3458. (l) Gott, A. L.; McGowan, P. C.; Temple, C. N. *Organometallics* **2008**, *27*, 2852.
- (15) For example, see: (a) Moreland, A. C.; Rauchfuss, T. B. *Inorg. Chem.* **2000**, *39*, 3029. (b) Blakesley, D. W.; Payne, S. C.; Hagen, K. S. *Inorg. Chem.* **2000**, *39*, 1979. (c) Enomoto, M.; Aida, T. *J. Am. Chem. Soc.* **2002**, *124*, 6099. (d) Gott, A. L.; McGowan, P. C.; Podesta, T. J.; Thornton-Pett, M. *J. Chem. Soc., Dalton Trans.* **2002**, 3619. (e) Slep, L. D.; Mijovilovich, A.; Meyer-Klaucke, W.; Weyhermüller, T.; Bill, E.; Bothe, E.; Neese, F.; Wieghardt, K. *J. Am. Chem. Soc.* **2003**, *125*, 15554. (f) Komuro, T.; Matsuo, T.; Kawaguchi, H.; Tatsumi, K. *Inorg. Chem.* **2003**, *42*, 5340. (g) Roelfes, G.; Vrajmasu, V.; Chen, K.; Ho, R. Y. N.; Rohde, J.-U.; Zondervan, C.; la Crois, R. M.; Schudde, E. P.; Lutz, M.; Spek, A. L.; Hage, R.; Feringa, B. L.; Münck, E.; Que, L., Jr. *Inorg. Chem.* **2003**, *42*, 2639. (h) Gott, A. L.; McGowan, P. C.; Podesta, T. J.; Tate, C. W. *Inorg. Chim. Acta* **2004**, *357*, 689. (i) Song, Y.-F.; Berry, J. F.; Bill, E.; Bothe, E.; Weyhermüller, T.; Wieghardt, K. *Inorg. Chem.* **2007**, *46*, 2208.
- (16) For example, see: (a) Yang, S.-M.; Cheng, W.-C.; Peng, S.-M.; Cheung, K.-K.; Che, C.-M. *J. Chem. Soc., Dalton Trans.* **1995**, 2955. (b) Yang, S.-M.; Chan, M. C.-W.; Cheung, K.-K.; Che, C.-M.; Peng, S.-M. *Organometallics* **1997**, *16*, 2819. (c) Au, S.-M.; Zhang, S.-B.; Fung, W.-H.; Yu, W.-Y.; Che, C.-M.; Cheung, K.-K. *Chem. Commun.* **1998**, 2677. (d) Che, C.-M.; Yu, W.-Y.; Chan, P.-M.; Cheng, W.-C.; Peng, S.-M.; Lau, K.-C.; Li, W.-K. *J. Am. Chem. Soc.* **2000**, *122*, 11380. (e) Cheung, W.-H.; Yu, W.-Y.; Yip, W.-P.; Zhu, N.-Y.; Che, C.-M. *J. Org. Chem.* **2002**, *67*, 7716. (f) Cameron, B. R.; Darks, M. C.; Baird, I. R.; Skerlj, R. T.; Santucci, Z. L.; Fricker, S. P. *Inorg. Chem.* **2003**, *42*, 4102. (g) Yip, W.-P.; Yu, W.-Y.; Zhu, N.; Che, C.-M. *J. Am. Chem. Soc.* **2005**, *127*, 14239. (h) Yip, W.-P.; Ho, C.-M.; Zhu, N.; Lau, T.-C.; Che, C.-M. *Chem. Asian J.* **2008**, *3*, 70.
- (17) (a) Ng, S. M.; Fang, Y. Q.; Lau, C. P.; Wong, W. T.; Jia, G. *Organometallics* **1998**, *17*, 2052. (b) Gott, A. L.; McGowan, P. C.; Podesta, T. J. *Dalton Trans.* **2008**, 3729.
- (18) (a) Ware, D. C.; Olmstead, M. M.; Wang, R.; Taube, H. *Inorg. Chem.* **1996**, *35*, 2576. (b) Wang, R.; Eberspacher, T. A.; Hasegawa, T.; Day, V.; Ware, D. C.; Taube, H. *Inorg. Chem.* **2001**, *40*, 593.
- (19) (a) Schröder, M. *Pure Appl. Chem.* **1988**, *60*, 517. (b) Robinson, P. D.; Ali, I. A.; Hinchley, C. C. *Acta Crystallogr.* **1991**, *C47*, 651.

Scheme 1



and spectroscopic features with those of the Tp and Cp counterparts. This paper reports, in addition to the results of this study, a new entry to osmium chemistry with triamine ligands, which allows the preparation of trihydride–dihydride–dihydrogen, and bis(dihydrogen) derivatives.

Results and Discussion

1. TACN Complexes. A method of general use in preparing compounds containing a Cp ligand in OsP^iPr_3 chemistry involves the reaction between the precursor $\text{OsH}_2\text{Cl}_2(\text{P}^i\text{Pr}_3)_2$ ²⁰ and a Cp derivative of an s- or p-block element.²¹ However, this method is not useful in generating the related IndOs compounds (Ind = indenyl). The entry into the latter takes place via the complex $\text{OsH}(\text{Ind})(\text{P}^i\text{Pr}_3)_2$, which is prepared in high yield by the reaction of trihydride $\text{OsH}_3\text{Cl}(\text{P}^i\text{Pr}_3)_2$ ²² (**1**) with LiInd.²³ Complex **1** has also shown to be a suitable precursor to the synthesis of $\text{OsH}_3\text{Tp}(\text{P}^i\text{Pr}_3)$, which is allowing the development of OsTp chemistry.^{8a,12} With these precedents in mind, we decided to explore the reaction of **1** with TACN, as a method to coordinate the triamine to the OsP^iPr_3 unit.

The treatment at 60 °C for 12 h of a toluene solution of **1** with 1.2 equiv of TACN leads to the monocationic trihydride derivative $[\text{OsH}_3(\text{TACN})(\text{P}^i\text{Pr}_3)]\text{Cl}$ (**2**), which is isolated as a white solid in 70% yield, according to Scheme 1. Its formation is the result of the displacement of the chloride anion and one of the phosphine groups of **1** by the triamine ligand.

Figure 1 shows a molecular diagram of the cation of **2**, obtained from X-ray diffraction data. The structure proves the coordination of the amine, which, as expected, acts as a tripodal facial $\kappa^3\text{-N,N,N}$ ligand. Thus, the geometry around the osmium atom can be rationalized as a distorted pentagonal bipyramid of C_s symmetry, with the phosphine ligand and the N(1)-TACN atom occupying axial positions [$\text{P}(1)\text{---Os---N}(1) = 178.67(10)^\circ$]. The metal coordination sphere is completed by the hydride ligands and the nitrogen atoms N(2) and N(3) of the TACN group lying in the base. This ligand distribution is similar to that found in the related Tp derivative $\text{OsH}_3\text{Tp}(\text{P}^i\text{Pr}_3)$. However, it should be noted that the $\text{N}_{\text{meridional}}\text{---Os---N}_{\text{meridional}}$ angle

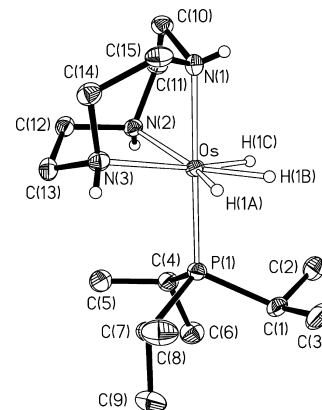


Figure 1. Molecular diagram of the cation of **2**. Thermal ellipsoids are shown at 50%.

Table 1. Selected Bond Lengths (Å) and Angles (deg) of Complexes **2**, **2t**, **4**, **4t**, **6**, and **6t**

	2	2t	4	4t	6	6t
Os–N(1)	2.174(3)	2.183	2.183(3)	2.195	2.179(3)	2.180
Os–N(2)	2.192(4)	2.220	2.176(3)	2.205	2.206(3)	2.253
Os–N(3)	2.192(4)	2.219	2.216(3)	2.236	2.210(3)	2.233
Os–P(1)	2.2637(11)	2.315	2.2708(10)	2.325	2.2652(9)	2.321
Os–H(1A)	1.583(10)	1.620	1.51(4)	1.619	1.591(10)	1.615
Os–H(1B)	1.576(10)	1.597	1.52(4)	1.598	1.579(10)	1.590
Os–H(1C)	1.585(10)	1.622	1.39(4)	1.623	1.583(10)	1.620
H(1A)–H(1B)		1.583		1.585		1.593
H(1B)–H(1C)		1.611		1.622		1.541
N(1)–Os–N(2)	78.62(13)	78.18	79.71(11)	79.35	78.73(11)	78.21
N(1)–Os–N(3)	78.13(13)	78.02	84.33(11)	84.63	78.95(11)	79.15
N(2)–Os–N(3)	77.66(13)	77.08	78.28(11)	78.36	82.64(11)	85.65
N(1)–Os–P(1)	178.67(10)	176.40	174.86(8)	174.36	176.47(9)	177.38
N(2)–Os–P(1)	102.71(10)	103.85	103.19(8)	104.17	102.82(8)	104.34
N(3)–Os–P(1)	102.15(10)	105.27	100.36(8)	100.33	98.05(8)	100.33
H(1A)–Os–H(1B)	57(2)	58.97	63(2)	59.04	59(2)	59.63
H(1B)–Os–H(1C)	60(2)	60.07	60(2)	60.45	57(2)	57.40

$\text{N}(2)\text{---Os---N}(3)$ of $77.66(13)^\circ$ (Table 1) and the $\text{N}_{\text{meridional}}\text{---Os---N}_{\text{axial}}$ angles $\text{N}(1)\text{---Os---N}(2)$ and $\text{N}(1)\text{---Os---N}(3)$ of $78.62(13)^\circ$ and $78.13(13)^\circ$, respectively, are smaller than the related parameters in the Tp counterpart [$83.17(12)^\circ$, $84.71(12)^\circ$, and $83.49(12)^\circ$].

The hydride positions obtained from X-ray diffraction data are, in general, imprecise. However, density functional theory (DFT) calculations have been shown to provide useful accurate data for the hydrogen positions in both classical polyhydride and dihydrogen complexes.²⁴ Thus, to confirm the positions of the hydrogen atoms of **2** bonded to the metal center, the DFT/B3PW91 optimization of the structure of **2** was performed (**2t**, Figure 2). The OsH_3 unit adopts a disposition of local C_{2v} symmetry with $\text{H}(1\text{A})\text{---Os---H}(1\text{B})$ and $\text{H}(1\text{B})\text{---Os---H}(1\text{C})$ angles of 58.97° and 60.07° [$57(2)^\circ$ and $60(2)^\circ$ by X-ray diffraction], respectively, which agree well with those obtained for the optimized structure of the model Tp compounds $\text{OsH}_3\text{Tp}(\text{P}^i\text{Pr}_3)$ (60.0° and 59.9°).¹² However, they are smaller than those determined by X-ray diffraction analysis for the $C_5\text{Me}_5$ derivatives $\text{OsH}_3(\eta^5\text{-C}_5\text{Me}_5)(\text{AsPh}_3)$ [$60(3)^\circ$ and $70(3)^\circ$] and $\text{OsH}_3(\eta^5\text{-C}_5\text{Me}_5)(\text{PPh}_3)$ [$64(2)^\circ$ and $68(2)^\circ$], which show four-legged piano-

(20) Aracama, M.; Esteruelas, M. A.; Lahoz, F. J.; López, J. A.; Meyer, U.; Oro, L. A.; Werner, H. *Inorg. Chem.* **1991**, *30*, 288.

(21) (a) Esteruelas, M. A.; López, A. M.; Ruiz, N.; Tolosa, J. I. *Organometallics* **1997**, *16*, 4657. (b) Esteruelas, M. A.; López, A. M.; Oñate, E.; Royo, E. *Organometallics* **2004**, *23*, 3021. (c) Esteruelas, M. A.; López, A. M.; Oñate, E.; Royo, E. *Organometallics* **2004**, *23*, 5633. (d) Esteruelas, M. A.; López, A. M. *Organometallics* **2005**, *24*, 3584.

(22) Gusev, D. G.; Kuhlman, R.; Sini, G.; Eisenstein, O.; Caulton, K. G. *J. Am. Chem. Soc.* **1994**, *116*, 2685.

(23) Esteruelas, M. A.; López, A. M.; Oñate, E.; Royo, E. *Organometallics* **2005**, *24*, 5780.

(24) (a) Zhao, D.; Bau, R. *Inorg. Chim. Acta* **1998**, *269*, 162. (b) Maseras, F.; Lledós, A.; Clot, E.; Eisenstein, O. *Chem. Rev.* **2000**, *100*, 601. (c) Barrio, P.; Esteruelas, M. A.; Lledós, A.; Oñate, E.; Tomàs, J. *Organometallics* **2004**, *23*, 3008.

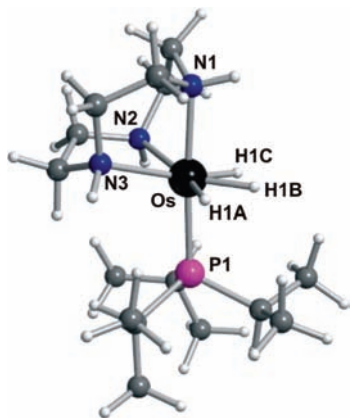


Figure 2. DFT/B3PW91-optimized geometry of **2t**.

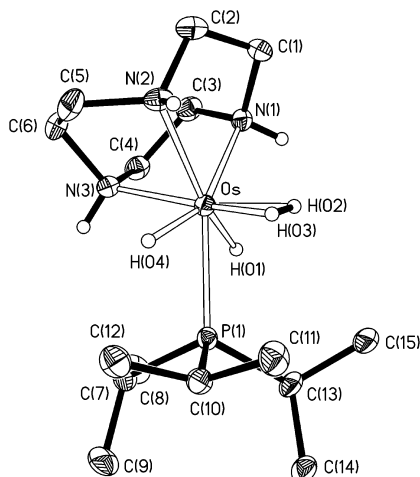


Figure 3. Molecular diagram of the cation of **3**. Thermal ellipsoids are shown at 50%.

stool structures.²⁵ The Os–H bond lengths for the terminal hydrogen atoms H(1A) and H(1C) are almost identical, 1.620 and 1.622 Å, respectively, whereas the central hydride H(1B) lies 1.597 Å away from the metal. The separations between the latter atom and those of the corners are 1.583 Å [H(1A)–H(1B)] and 1.611 Å [H(1B)–H(1C)].

The most noticeable spectroscopic features of **2** are a singlet at 33.2 ppm in the $^{31}\text{P}\{^1\text{H}\}$ NMR spectrum and a doublet at –12.28 ppm, with a H–P coupling constant of 15.6 Hz, in the ^1H NMR spectrum. The presence at room temperature of only one resonance for the 2:1 inequivalent hydride ligands indicates that the hydride atoms bonded to osmium undergo a thermally activated site-exchange process. Lowering the sample temperature produces a broadening of the resonance. However, decoalescence is not observed down to 193 K. The T_1 values of this resonance were determined at 300 MHz over the temperature range 273–193 K. A $T_{1(\text{min})}$ value of 80 ± 1 ms was obtained at 213 K.

The total relaxation rate for each H(*n*) hydride ligand ($R_{\text{H}(n)} = 1/T_{1(\text{min})\text{H}(n)}$) of **2** is the addition of the relaxation rate due to the hydride–hydride and hydride–hydrogen of the NH group dipole–dipole interactions (at 300 MHz, $R_{\text{H–H}} = 129.18/r_{\text{HH}}^6$ and $R_{\text{H–H}'} = 129.18/r_{\text{HH}'}$, respectively) and that

(25) Gross, C. L.; Girolami, G. S. *Organometallics* **2006**, *25*, 4792.

Table 2. Selected Bond Lengths (Å) and Angles (deg) of Complexes **3** and **3t**

Os–N(1)	2.154(5)	2.179
Os–N(2)	2.171(4)	2.189
Os–N(3)	2.146(5)	2.156
Os–P(1)	2.3312(14)	2.420
Os–H(01)	1.577(10)	1.624
Os–H(02)	1.582(10)	1.650
Os–H(03)	1.582(10)	1.651
Os–H(04)	1.578(10)	1.617
H(01)–H(02)		2.059
H(02)–H(03)	0.86(9)	1.033
H(03)–H(04)		2.086
N(1)–Os–N(2)	77.43(17)	77.50
N(1)–Os–N(3)	78.74(18)	79.02
N(2)–Os–N(3)	79.26(17)	79.03
N(1)–Os–P(1)	143.00(12)	143.76
N(2)–Os–P(1)	139.57(13)	138.68
N(3)–Os–P(1)	104.52(13)	105.87
H(01)–Os–H(02)	79(3)	77.94
H(02)–Os–H(03)	32(3)	36.46
H(03)–Os–H(04)	84(4)	79.29

due to all other relaxation contributors (R^*),²⁶ which can be estimated to be 1.2 s^{-1} ,²⁷ a value similar to those found for the related trihydride compounds $[\text{OsH}_3(\text{diolofin})(\text{P}^i\text{Pr}_3)_2]\text{BF}_4$.²⁸ Thus, one can obtain values of R_{H} converted to the 300 MHz scale for each hydride ligand by using eqs 1–3, once the structure of **2** is known and the separations between hydrides (r_{HH}) and between the hydrides and the NH hydrogens of the TACN ligand ($r_{\text{HH}'}$) have been optimized.

$$R_{\text{H}(1\text{A})} = R^* + R_{\text{H}(1\text{A})-\text{H}(1\text{B})} + R_{\text{H}(1\text{A})-\text{H}(1\text{C})} + R_{\text{H}(1\text{A})-\text{H}'(1\text{A})} + R_{\text{H}(1\text{A})-\text{H}'(1\text{B})} + R_{\text{H}(1\text{A})-\text{H}'(1\text{C})} \quad (1)$$

$$R_{\text{H}(1\text{B})} = R^* + R_{\text{H}(1\text{B})-\text{H}(1\text{A})} + R_{\text{H}(1\text{B})-\text{H}(1\text{C})} + R_{\text{H}(1\text{B})-\text{H}'(1\text{A})} + R_{\text{H}(1\text{B})-\text{H}'(1\text{B})} + R_{\text{H}(1\text{B})-\text{H}'(1\text{C})} \quad (2)$$

$$R_{\text{H}(1\text{C})} = R^* + R_{\text{H}(1\text{C})-\text{H}(1\text{A})} + R_{\text{H}(1\text{C})-\text{H}(1\text{B})} + R_{\text{H}(1\text{C})-\text{H}'(1\text{A})} + R_{\text{H}(1\text{C})-\text{H}'(1\text{B})} + R_{\text{H}(1\text{C})-\text{H}'(1\text{C})} \quad (3)$$

For exchange rates higher than 100 s^{-1} , as in this case at 213 K, the relaxation rate is the weighted average of the relaxation rate of each hydride (eq 4).²⁹

$$R = [R_{\text{H}(1\text{A})} + R_{\text{H}(1\text{B})} + R_{\text{H}(1\text{C})}]/3 \quad (4)$$

Solving $R_{\text{H}(1\text{A})}$, $R_{\text{H}(1\text{B})}$, and $R_{\text{H}(1\text{C})}$ yields an R value of 12.4 s^{-1} , which leads to a $T_{1(\text{min})}$ value of 81 ms in good agreement with that determined by ^1H NMR spectroscopy.

Complex **2** is a Brønsted base in spite of its cationic character. The addition at room temperature of 4.8 equiv of HBF_4 to a dichloromethane solution of the trihydride gives rise to the formation of $[\text{OsH}_2(\text{TACN})(\eta^2\text{-H}_2)(\text{P}^i\text{Pr}_3)](\text{BF}_4)_2$ (**3**), as a consequence of the protonation of the starting cation. This dicationic dihydride–dihydrogen derivative is isolated as a white solid in 82% yield, according to Scheme 1.

Complex **3** has also been characterized by X-ray diffraction analysis. Figure 3 shows a view of the structure, whereas selected bond lengths and angles are given in Table 2. Like

(26) Baya, M.; Eguillor, B.; Esteruelas, M. A.; Oliván, M.; Oñate, E. *Organometallics* **2007**, *26*, 6556, and references cited therein.

(27) This value affords the best compromise between the experimental $T_{1(\text{min})}$ values of **2**, **4**, and **6** and those calculated from **2t**, **4t**, and **6t**.

(28) Castillo, A.; Esteruelas, M. A.; Oñate, E.; Ruiz, N. *J. Am. Chem. Soc.* **1997**, *119*, 9691.

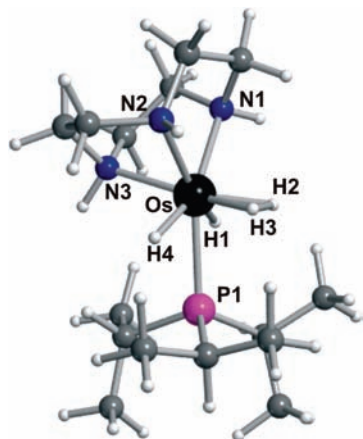


Figure 4. DFT/B3PW91-optimized geometry of **3t**.

Table 3. Selected NMR Data of Complexes **3**, **5**, **7**, and $[\text{OsTp}(\eta^2\text{-H}_2)_2(\text{P}^i\text{Pr}_3)]^+$

complex	^1H				$^{31}\text{P}\{^1\text{H}\}$	
	$\delta_{\text{Os-H}(\text{OsH}_4)}$	J_{HP}	$T_1(\text{exp})$	J_{HD}	δ	$\Delta\delta_{\text{OsH}_3\text{-OsH}_4}$
3	−9.07	19.8	24	3.0	52.6	19.4
5	−9.11	19.8	23	3.0	51.3	21.6
7	−10.31	8.1	14		32.5	−6.5
$[\text{OsH}_4\text{Tp}(\text{P}^i\text{Pr}_3)]^+$	−8.45	7.2	12		20.2	−8.5

in **2**, the geometry around the osmium atom can be described as a distorted pentagonal bipyramid of C_s symmetry. However, in this case the axial positions are occupied by the H(02)–H(03) dihydrogen ligand and the N(3)-TACN atom. The base of the pyramid is formed by the nitrogen atoms N(1) and N(2) of the TACN amine cisoid-disposed to the H(01) and H(04) hydride ligands, respectively, and the phosphine group situated between the hydrides. The $N_{\text{meridional}}\text{-Os-}N_{\text{meridional}}$ angle N(1)–Os–N(2) of $77.43(17)^\circ$ and the $N_{\text{meridional}}\text{-Os-}N_{\text{axial}}$ angles N(1)–Os–N(3) and N(2)–Os–N(3) of $78.74(18)^\circ$ and $79.26(17)^\circ$, respectively, agree well with those of **2**.

The dihydride–dihydrogen nature of **3** was confirmed by means of optimization of the obtained X-ray structure at the DFT/B3PW91 level of theory (**3t**, Figure 4). The H(02)–H(03) distance of 1.033 Å is similar to the dihydrogen bond lengths determined from neutron diffraction data³⁰ for the C_5Me_5 complexes $[\text{OsH}_2(\eta^5\text{-C}_5\text{Me}_5)(\eta^2\text{-H}_2)(\text{PPh}_3)]^+$ [1.01(1) Å] and $[\text{OsH}_2(\eta^5\text{-C}_5\text{Me}_5)(\eta^2\text{-H}_2)(\text{AsPh}_3)]^+$ [1.08(1) Å] and about 0.3 Å shorter than that in $[\text{OsH}_2(\eta^5\text{-C}_5\text{Me}_5)(\eta^2\text{-H}_2)(\text{PCy}_3)]^+$ [1.31(3) Å].

The $^{31}\text{P}\{^1\text{H}\}$ NMR spectrum of **3** contains a singlet at 52.6 ppm, which is shifted by 19.4 ppm to lower field with regard to that of **2** (Table 3). At room temperature, the ^1H NMR spectrum in acetonitrile- d_3 shows at −9.07 ppm a doublet with a H–P coupling constant of 19.8 ppm. The presence of only one resonance for the equivalent hydride ligands and the coordinate hydrogen molecule indicates that exchange of the classical and nonclassical hydrogen atom sites is fast on the NMR time scale. Lowering the sample temperature produces a broadening of the resonance. However, decoa-

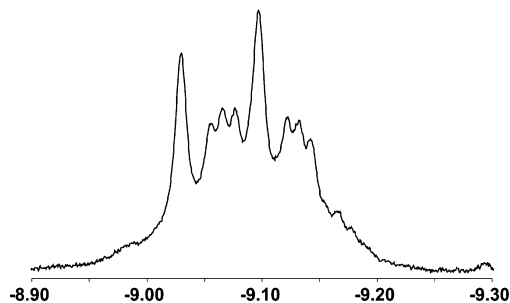


Figure 5. Hydride region of the 300 MHz ^1H NMR spectrum of the reaction of **2** with 1.5 equiv of trifluoromethanesulfonic acid- d_1 , at 298 K in acetonitrile- d_3 .

lence is not observed down to 198 K in a 2:1 $\text{CDCl}_2/\text{CD}_3\text{CN}$ mixture.

Additional insight into the solution structure is obtained from the ^1H NMR spectrum of the partially deuterated isotopologues of **3** (Figure 5), which are generated by the addition of 1.5 equiv of trifluoromethanesulfonic acid- d_1 to an acetonitrile- d_3 solution of **2**. The multiplet splitting gives a H–D coupling constant of 3.0 Hz. This value is average owing to the exchange process in the OsH_4 unit. If we assume that there is no site preference for the hydrogen and deuterium atoms, the average coupling constant is equal to $[^1J_{\text{HD}} + 4(^2J_{\text{HD}}) + ^2J'_{\text{HD}}]/6$ where $^1J_{\text{HD}}$, $^2J_{\text{HD}}$, and $^2J'_{\text{HD}}$ are the couplings within the dihydrogen ligand, between the dihydrogen atoms and the hydrides, and between both classical hydrides. If we adopt typical values for the geminal $^2J_{\text{HD}}$ couplings between −1 and +1 Hz,³¹ $^1J_{\text{HD}}$ is between 13.0 and 23.0 Hz. These values afford a H–H distance range between 0.95 and 1.22 Å,³² which contains the H–H distance obtained by DFT calculations.

The behavior of **2** is similar to the behavior of the Cp counterpart $\text{OsH}_3\text{Cp}(\text{P}^i\text{Pr}_3)$. In contrast to the Tp analogue $\text{OsH}_3\text{Tp}(\text{P}^i\text{Pr}_3)$, which generates a bis-dihydrogen derivative,¹² both species afford dihydride–dihydrogen compounds by protonation. These facts indicate that (i) the charge is not determinant for the dihydride or dihydrogen nature of the complex and (ii) the abilities of the TACN and Cp ligands to stabilize dihydrogen derivatives are similar and lower than that of the Tp group.

The scarce influence of the charge on the interactions between the hydrogen atoms bonded to the metal center has precedent in ruthenium chemistry. Although the dihydrogen $[\text{Ru}(\text{TACN})(\eta^2\text{-H}_2)(\text{CO})(\text{PPh}_3)]^{2+}$ and $[\text{Ru}(\text{TACN})(\eta^2\text{-H}_2)(\text{PPh}_3)_2]^{2+}$ complexes are dicationic and the Tp analogues monocationic, $^1J_{\text{HD}}$ coupling of the isotopomers of the TACN compounds is smaller than those of the Tp counterparts. On the other hand, in contrast to osmium, the ability of the TACN ligand to stabilize nonclassical structures in ruthenium

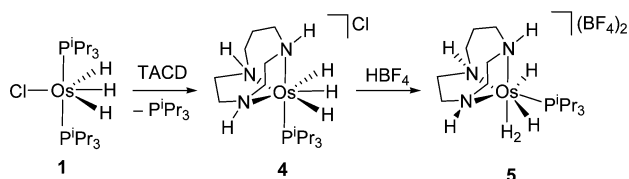
(31) Gross, C. L.; Girolami, G. S. *Organometallics* **2007**, *26*, 1658.

(32) The calculated range undergoes slight variations depending upon the equation used: 0.95–1.14 Å, according to Hush's equation (Hush, N. S. *J. Am. Chem. Soc.* **1997**, *119*, 1717), 0.98–1.18 Å, according to Limbach's equation (Gründemann, S.; Limbach, H.-H.; Buntkowski, G.; Sabo-Etienne, S.; Chaudret, B. *J. Phys. Chem. A* **1999**, *103*, 4752), 1.04–1.20 Å, according to Morris' equation (Maltby, P. A.; Schlaf, M.; Steinbeck, M.; Lough, A. J.; Morris, R. H.; Klooster, W. T.; Koetzle, T. F.; Srivastava, R. C. *J. Am. Chem. Soc.* **1996**, *118*, 5396), and 1.05–1.22 Å, according to Heinekey's equation (Luther, T. A.; Heinekey, D. M. *Inorg. Chem.* **1998**, *37*, 127).

(29) Desrosiers, P. J.; Cai, L.; Lin, Z.; Richards, R.; Halpern, J. *J. Am. Chem. Soc.* **1991**, *113*, 4173.

(30) Webster, C. E.; Gross, C. L.; Young, D. M.; Girolami, G. S.; Schultz, A. J.; Hall, M. B.; Eckert, J. *J. Am. Chem. Soc.* **2005**, *127*, 15091.

Scheme 2



chemistry is similar to that of the Tp group and higher than that of the Cp group. Thus, while $[\text{RuH}_2\text{Cp}(\text{PPh}_3)_2]^+$ is a classical dihydride complex, both $[\text{RuTp}(\eta^2\text{-H}_2)(\text{PPh}_3)_2]^{2+}$ and $[\text{Ru}(\text{TACN})(\eta^2\text{-H}_2)(\text{PPh}_3)_2]^{2+}$ are dihydrogen derivatives.^{17a}

2. TACD Complexes. The difference in behavior between **2** and its Tp counterpart is consistent with the difference observed in the N–Os–N angles of both compounds. While the N–Os–N angles of **2** are close to 78° , those of the Tp compound are close to 84° , a value near 90° . In order to approach one of the N–Os–N angles of these triamine systems to the angles of the Tp complex, we have carried out the reaction of **1** with TACD, which has an additional CH_2 spacer between two of the NH groups.

The treatment at 60°C for 12 h of a toluene solution of **1** with 1.1 equiv of TACD leads to the trihydride $[\text{OsH}_3(\text{TACD})(\text{P}^i\text{Pr}_3)]\text{Cl}$ (**4**), which is isolated as a white solid in 70% yield, according to Scheme 2.

Figure 6 shows a view of the structure of **4**, whereas selected bond lengths and angles are given in Table 1. As expected, the geometry around the metal center is similar to that of **2**, i.e., a pentagonal bipyramid with the phosphine and the nitrogen atom N(1) in axial positions and the hydride ligands and the nitrogen atoms N(2) and N(3) in the base. The trimethylene group $\text{C}(5)\text{H}_2\text{-C}(6)\text{H}_2\text{-C}(7)\text{H}_2$ separates the equatorial nitrogen atom N(3) and the axial nitrogen atom N(1) and breaks the C_s symmetry of the bipyramid. As a consequence of this, the $N_{\text{meridional}}\text{-Os-}N_{\text{axial}}$ angle N(1)–Os–N(3) is opened up to $84.33(11)^\circ$, while the other $N_{\text{meridional}}\text{-Os-}N_{\text{axial}}$ angle N(1)–Os–N(2) [$79.71(11)^\circ$] and the $N_{\text{meridional}}\text{-Os-}N_{\text{meridional}}$ angle N(2)–Os–N(3) [$78.28(11)^\circ$] remain close to 78° .

The asymmetry of the cation has no significant influence on the structural parameters of the OsH_3 unit. The DFT/

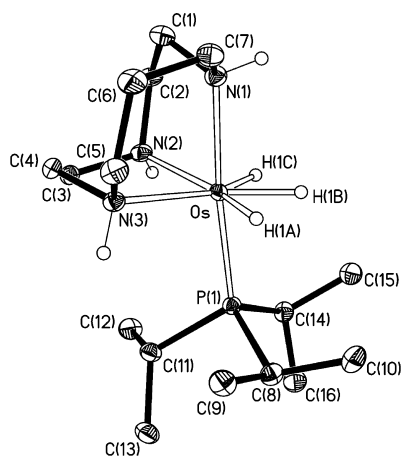


Figure 6. Molecular diagram of the cation of **4**. Thermal ellipsoids are shown at 50%.

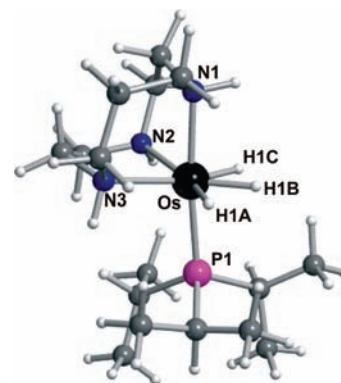


Figure 7. DFT/B3PW91-optimized geometry of **4t**.

B3PW91 optimization of the structure (**4t**, Figure 7) provides hydrogen–hydrogen separations of 1.585 \AA [$\text{H}(1\text{A})\text{-H}(1\text{B})$] and 1.622 \AA [$\text{H}(1\text{B})\text{-H}(1\text{C})$] and $\text{H}(1\text{A})\text{-Os-}H(1\text{B})$ and $\text{H}(1\text{B})\text{-Os-}H(1\text{C})$ angles of 59.04 and 60.45° , respectively, which are very similar to the ones calculated for **2**.

The $^1\text{H}\{^{31}\text{P}\}$ NMR spectrum of **4** in dichloromethane- d_2 at 203 K is consistent with the structures shown in Figures 6 and 7. Thus, in agreement with the presence in the cation of three inequivalent hydride ligands, it contains an ABC spin system in the high-field region, defined by $\delta_{\text{A}} = -11.1$ ppm, $\delta_{\text{B}} = -12.1$ ppm, and $\delta_{\text{C}} = -13.2$ ppm and $J_{\text{AB}} = 117$ Hz, $J_{\text{BC}} = 65$ Hz, and $J_{\text{AC}} = 0$ Hz. The large values of J_{AB} and J_{BC} suggest the operation of quantum exchange coupling³³ between the central hydride H_{B} and those of the corners. This is supported by the spectrum at 193 K, which shows J_{AB} and J_{BC} values of 99 and 59 Hz, respectively. At room temperature in acetonitrile- d_3 , the spectrum contains a singlet at -12.06 ppm, which is converted into a doublet with a H–P coupling constant of 15.9 Hz in the ^1H NMR spectrum. This signal indicates that the hydride ligands also undergo a thermally activated site-exchange process. A singlet at 29.7 ppm in the $^{31}\text{P}\{^1\text{H}\}$ NMR spectrum is another characteristic feature of **4**.

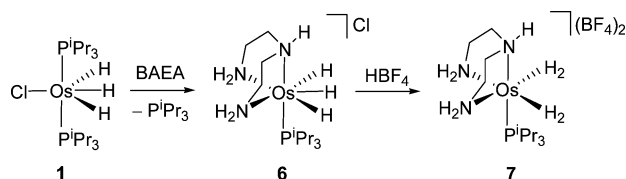
The presence of a $N_{\text{meridional}}\text{-Os-}N_{\text{axial}}$ angle in **4** close to 84° , and therefore similar to those of the Tp counterpart, does not modify its behavior with regard to that of **2**. The addition at room temperature of 3.7 equiv of HBF_4 to a dichloromethane solution of **4** leads to the dihydride–dihydrogen derivative $[\text{OsH}_2(\text{TACD})(\eta^2\text{-H}_2)(\text{P}^i\text{Pr}_3)](\text{BF}_4)_2$ (**5**) analogue to **3**, which is isolated as a white solid in 82% yield, according to Scheme 2.

The relevant spectroscopic data of **5** are almost identical with those of **3** (Table 3). The $^{31}\text{P}\{^1\text{H}\}$ NMR spectrum contains a singlet at 51.3 ppm, shifted by 21.6 ppm to lower field with regard to that of **4**. At room temperature, the ^1H NMR spectrum in acetonitrile- d_3 shows at -9.11 ppm a doublet with a H–P coupling constant of 19.8 Hz. The J_{HD} coupling constant in the partially deuterated isotopologues is 3.0 Hz, the same value as that in **3**. The $T_{1(\text{min})}$ value of 23 ± 1 ms, found at 213 K, is also similar to that of **3**.

3. BAEA Complexes. In order to open selectively the $N_{\text{meridional}}\text{-Os-}N_{\text{meridional}}$ angle of the pyramid, we have selected the BAEA triamine. This group would allow us to

(33) Sabo-Etienne, S.; Chaudret, B. *Chem. Rev.* **1998**, *98*, 2077.

Scheme 3



keep the C_s symmetry of the cation, without imposing restrictions on the $N_{\text{meridional}}\text{—Os—}N_{\text{meridional}}$ angle because $N_{\text{terminal}}\text{—M—}N_{\text{terminal}}$ angles between 78 and 164° have been reported for this ligand.³⁴

The treatment at 60°C for 12 h of a toluene solution of **1** with 1.7 equiv of BAEA leads to the trihydride $[\text{OsH}_3(\text{BAEA})(\text{P}^i\text{Pr}_3)]\text{Cl}$ (**6**), which is isolated in 62% yield, according to Scheme 3.

Figure 8 shows a view of the structure of **6**. Selected bond lengths and angles are given in Table 1. The geometry around the metal center is the expected one: a pentagonal bipyramid of C_s symmetry with the phosphine and the bridge nitrogen atom N(1) of the triamine in axial positions [$\text{P}(1)\text{—Os—}N(1) = 176.47(9)^\circ$]. The base is formed by the terminal nitrogen atoms N(2) and N(3) and the hydride ligands. Both $N_{\text{axial}}\text{—Os—}N_{\text{meridional}}$ angles $N(1)\text{—Os—}N(2)$ and $N(1)\text{—Os—}N(3)$ of $78.73(11)^\circ$ and $78.95(11)^\circ$ are similar to those of **2**, while the $N_{\text{meridional}}\text{—Os—}N_{\text{meridional}}$ angle $N(2)\text{—Os—}N(3)$ of $82.64(11)^\circ$ is close to the related angle in the Tp counterpart and near 90° .

The opening of the $N_{\text{meridional}}\text{—Os—}N_{\text{meridional}}$ angle of the pyramid appears to provoke the approach of H(1C) to H(1B). Thus, the separation between these hydride ligands of 1.541 \AA , obtained from the DFT/B3PW91 optimization of the structure of **6** (**6t**, Figure 9) is between 0.07 and 0.08 \AA shorter than those calculated for **2t** and **4t**. In contrast to the H(1B)—H(1C) distance, the separation between H(1A) and H(1B) of 1.593 \AA is very similar to those in the cyclic triamine complexes.

The NMR spectra of **6** agree well with those of **2**. The $^{31}\text{P}\{^1\text{H}\}$ NMR spectrum in acetonitrile- d_3 contains a singlet at 39.0 ppm . In the ^1H NMR spectrum at room temperature, the hydride ligands display at -12.38 ppm a doublet with a H—P coupling constant of 14.7 Hz , in agreement with the operation of a thermally activated site-exchange process. Lowering the sample temperature produces a broadening of the resonance. However, decoalescence is not observed down to 193 K . The $300\text{ MHz } T_1$ study of this resonance, over the temperature range $273\text{—}193\text{ K}$, affords a $T_{1(\text{min})}$ value of $77 \pm 1\text{ ms}$ at 203 K , which is consistent with the structural parameters of **6t**.

In contrast to $N_{\text{meridional}}\text{—Os—}N_{\text{axial}}$ angles, the $N_{\text{meridional}}\text{—Os—}N_{\text{meridional}}$ angle of the pyramid certainly has a significant influence on the chemistry of these trihydride complexes. Thus, there is a marked difference in the behavior between the cyclic triamine compounds **2** and **4**

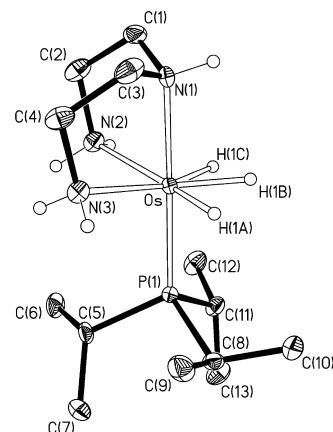


Figure 8. Molecular diagram of the cation of **6**. Thermal ellipsoids are shown at 50%.

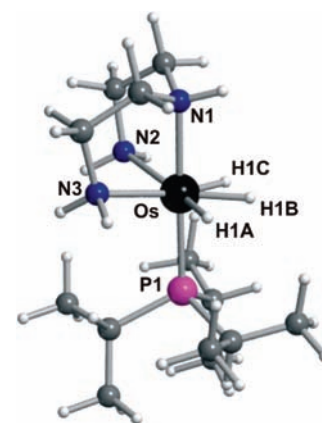


Figure 9. DFT/B3PW91-optimized geometry of **6t**.

and the BAEA derivative. Complex **6**, unlike **2** and **4**, reacts with HBF_4 in dichloromethane at room temperature to give the bis(dihydrogen) complex $[\text{Os}(\text{BAEA})(\eta^2\text{—H}_2)_2(\text{P}^i\text{Pr}_3)](\text{BF}_4)_2$ (**7**), which is isolated as a white solid in 90% yield, according to Scheme 3.

The relevant spectroscopic data of **7** agree well with those of the Tp counterpart $[\text{OsTp}(\eta^2\text{—H}_2)_2(\text{P}^i\text{Pr}_3)]\text{BF}_4$, where the bis(dihydrogen) nature of the complex has been proven by X-ray diffraction analysis and confirmed by DFT calculations,¹² and show notable differences with those of **3** and **5** (Table 3). Thus, at room temperature in acetonitrile- d_3 , the ^1H NMR spectrum shows at -10.31 ppm a doublet with a H—P coupling constant of 8.1 Hz , which is similar to the one observed in the Tp analogue (7.2 Hz) and 11.7 Hz smaller than those found in **3** and **5**. The $T_{1(\text{min})}$ value of this resonance, $14 \pm 1\text{ ms}$, is also similar to the value found for the resonance of the Tp complex ($12 \pm 1\text{ ms}$) and about 10 ms lower than those of the Os— H_4 resonances of **3** and **5**. The $^{31}\text{P}\{^1\text{H}\}$ NMR spectrum contains a singlet at 32.5 ppm , which, similarly to that of the Tp counterpart and in contrast to those of **3** and **5**, is shifted by 6.5 ppm toward higher field with regard to the resonance of **6**.

The DFT/B3PW91-optimized structure of the model cation $[\text{Os}(\text{BAEA})(\eta^2\text{—H}_2)_2(\text{PMe}_3)]^{2+}$ (**7t**, Figure 10) confirms the bis(dihydrogen) nature of the BAEA species. The geometry around the osmium atom can be described as a distorted octahedron with the terdentate ligand occupying *fac* positions.

(34) For example, see: (a) Chin, R. M.; Barrera, J.; Dubois, R. H.; Helberg, L. E.; Sabat, M.; Bartucz, T. Y.; Lough, A. J.; Morris, R. H.; Harman, W. D. *Inorg. Chem.* **1997**, *36*, 3553. (b) Stähler, R.; Näther, C.; Bensch, W. *Eur. J. Inorg. Chem.* **2001**, 1835. (c) Barth, M.; Kästele, Y.; Klüfers, P. *Eur. J. Inorg. Chem.* **2005**, 1353.

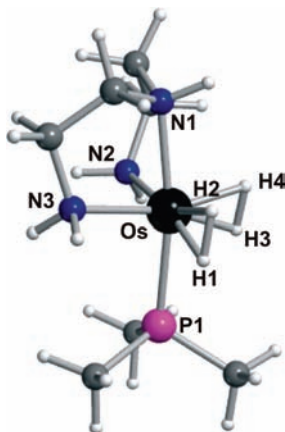


Figure 10. DFT/B3PW91-optimized geometry of **7t**. Selected bond lengths (Å) and angles (deg): Os–N(1) 2.192, Os–N(2) 2.170, Os–N(3) 2.159, Os–P(1) 2.412, Os–H(1) 1.673, Os–H(2) 1.669, Os–H(3) 1.674, Os–H(4) 1.668, H(1)–H(2) 0.974, H(3)–H(4), 0.968; N(1)–Os–N(2) 78.52, N(1)–Os–N(3) 78.99, N(2)–Os–N(3) 94.63, N(1)–Os–P(1) 170.20, N(2)–Os–P(1) 94.94, N(3)–Os–P(1) 94.43, H(1)–Os–H(2) 33.89, H(3)–Os–H(4) 33.69.

The coordinated hydrogen molecules are symmetrically disposed to the sides of the C_s symmetry plane of the cation. The H(1)–H(2) and H(3)–H(4) bond lengths are 0.974 and 0.968 Å, respectively. In addition, it should be noted that the $N_{\text{bridge}}\text{–Os–}N_{\text{terminal}}$ angles N(1)–Os–N(2) and N(1)–Os–N(3) of 78.52 and 78.99°, respectively, remain close to 78°, while $N_{\text{terminal}}\text{–Os–}N_{\text{terminal}}$ angle N(2)–Os–N(3) is opened up to 94.63°.

These results are consistent with observations of Girolami, Schultz, Hall, Eckert, and co-workers indicating that the nonclassical interactions in these types of systems are very sensitive to coligand–M–coligand angles in certain regions of the coordination sphere of the metal center because small changes in these angles can invert the relative energies of the metal orbitals presented to the bound H_2 .³⁰

Concluding Remarks. This paper shows an entry to the chemistry of osmium with cyclic and acyclic triamine ligands, which has afforded monocationic trihydride and dicationic dihydride–dihydrogen and bis(dihydrogen) derivatives. Furthermore, the systematical comparison of the structures and spectroscopic features of the new compounds and those of the Tp and Cp counterparts reveals that the charge of the complex has less influence on the interactions between the atoms of the OsH_n units than determined structural parameters, in particular some L–Os–L angles.

The starting point of the new chemistry is the trihydride $OsH_3Cl(P^iPr_3)_2$, which reacts with L_3 ligands such as TACN, TACD, and BAEA to afford the salts $[OsH_3L_3(P^iPr_3)]Cl$, characterized spectroscopically by X-ray diffraction analysis and DFT calculations. Like the neutral Tp counterpart, these compounds have structures that can be rationalized as pentagonal bipyramids with a nitrogen atom in the axial position and the other two lying in the base.

The $N_{\text{meridional}}\text{–Os–}N_{\text{meridional}}$ angle of the bipyramids determines the behavior of these species. The neutral Tp complex $OsH_3Tp(P^iPr_3)$, with an angle of 83.17(12)°, reacts with HBF_4 to give the monocationic bis(dihydrogen) derivative $[OsTp(\eta^2\text{-}H_2)_2(P^iPr_3)](BF_4)$.¹² However, the reactions of

the cationic TACN and TACD trihydrides, which have angles close to 78°, lead to the dicationic dihydride–dihydrogen compounds $[OsH_2(TACN)(\eta^2\text{-}H_2)(P^iPr_3)](BF_4)_2$ and $[OsH_2\text{-}(TACD)(\eta^2\text{-}H_2)(P^iPr_3)](BF_4)_2$, analogous to the Cp complex $[OsH_2Cp(\eta^2\text{-}H_2)(P^iPr_3)]BF_4$. In contrast to the trihydrides containing cyclic triamines, the BAEA trihydride with an angle similar to that of the Tp complex $OsH_3Tp(P^iPr_3)$, 82.5(3)°, reacts similarly to the latter to afford the dicationic bis(dihydrogen) $[Os(BAEA)(\eta^2\text{-}H_2)_2(P^iPr_3)](BF_4)_2$. Interestingly, DFT calculations on the model $[Os(BAEA)(\eta^2\text{-}H_2)_2(PMe_3)]^{2+}$ indicate that the N–Os–N angle of this dication, analogue to the $N_{\text{meridional}}\text{–Os–}N_{\text{meridional}}$ of the starting bipyramid, is opened up to 94.6°.

In conclusion, under the general statements rationalizing the nonclassical hydrogen–hydrogen interactions, there are facts concerning to the geometry of the L_nM fragments that subtly modify the combinations of metal orbitals interacting with the hydrogen molecules.

Experimental Section

General Methods and Instrumentation. All reactions were carried out under argon with rigorous exclusion of air using Schlenk-tube or glovebox techniques. Solvents were dried by the usual procedures and distilled under argon prior to use. The starting material $OsH_3Cl(P^iPr_3)_2$ (**1**) was prepared according to the published method.²² Bis(2-aminoethyl)amine (BAEA) and HBF_4 were obtained from commercial sources, whereas 1,4,7-triazacyclononane (TACN) and 1,4,7-triazacyclodecane (TACD) were prepared according to the published method.³⁵ NMR spectra were recorded on a Varian Gemini 2000, a Bruker ARX 300, or a Bruker Avance 300 MHz instrument, with resonating frequencies of 300 MHz (1H) and 121.5 MHz (^{31}P). Chemical shifts (expressed in parts per million) are referenced to residual solvent peaks (1H) or external H_3PO_4 (^{31}P). Coupling constants, J , are given in Hertz. IR spectra were run on a Perkin-Elmer Spectrum 100 FT-IR spectrometer. C, H, and N analyses were carried out on a Perkin-Elmer 2400 CHNS/O analyzer.

Preparation of $[OsH_3(TACN)(P^iPr_3)]Cl$ (2**).** To a brown toluene solution (15 mL) of **1**, generated in situ from $OsH_2Cl_2(P^iPr_3)_2$ (1098 mg, 1.88 mmol), molecular hydrogen, and triethylamine, was added TACN (305 mg, 2.36 mmol), and the resulting mixture was stirred for 12 h at 60 °C. The final yellow solution was concentrated to ca. 0.5 mL and pentane (6 mL) was added, causing the precipitation of a whitish solid. The precipitate was decanted, washed with pentane (4 × 8 mL), and dried in vacuo. An ivory solid was obtained. Yield: 690 mg (70%). Anal. Calcd for $C_{15}H_{39}ClN_3OsP$: C, 34.77; H, 7.59; N, 8.11. Found: C, 34.91; H, 7.60; N, 7.88. IR (cm^{-1}): 3219 (m, NH), 2088 (m, OsH). $^{31}P\{^1H\}$ NMR (CD_3CN , 298 K): δ 33.2 (s). 1H NMR (CD_3CN , 298 K): δ –12.28 (d, $^2J_{HP}$ = 15.6 Hz, 3 H, Os–H), 1.14 (dd, $^3J_{HP}$ = 12.6 Hz, $^3J_{HH}$ = 7.2 Hz, 18 H, PCHCH₃), 1.93 (m, 3 H, PCHCH₃), 2.77, 3.15 (m, 6 H each, NCH₂), 5.67 (br, 3 H, NH). $T_{1(\text{min})}$ (ms, OsH, CD_2Cl_2 , 213 K): 80 ± 1.

Preparation of $[OsH_2(TACN)(\eta^2\text{-}H_2)(P^iPr_3)](BF_4)_2$ (3**).** HBF_4 (1:1 solution in diethyl ether, 400 μ L, 2.93 mmol) was added to a dichloromethane (10 mL) suspension of **2** (315 mg, 0.61 mmol), and the mixture was stirred for 10 min. The resulting suspension was concentrated to ca. 3 mL, and diethyl ether (15 mL) was added. The solid was decanted, washed with diethyl ether (3 × 15 mL),

and dried in vacuo. A white solid was obtained. Yield: 329 mg (82%). Anal. Calcd for $C_{15}H_{40}B_2F_8N_3OsP$: C, 27.41; H, 6.13; N, 6.39. Found: C, 27.60; H, 6.18; N, 6.50. IR (cm^{-1}): 3301 (m, NH), 2150, 2095 (vw, OsH), 1006 (vs, BF_4^-). $^{31}P\{^1H\}$ NMR (CD_3CN , 298 K): δ 52.6 (s). 1H NMR (CD_3CN , 298 K): δ -9.07 (d, $^2J_{HP} = 19.8$ Hz, 4 H, Os–H), 1.25 (dd, $^3J_{HP} = 16.2$ Hz, $^3J_{HH} = 7.2$ Hz, 18 H, PCHCH₃), 2.44 (m, 3 H, PCHCH₃), 3.07, 3.36 (m, 6 H each, NCH₂), 6.44 (br, 3 H, NH). $T_{1(\min)}$ (ms, OsH, $CDCl_2F/CD_3CN$ (2:1), 213 K): 24 ± 1 .

Preparation of $[OsH_3(TACD)(P^iPr_3)Cl]$ (4). To a brown toluene solution (15 mL) of **1**, generated in situ from $OsH_2Cl_2(P^iPr_3)_2$ (1100 mg, 1.88 mmol), molecular hydrogen, and triethylamine, was added TACD (286 mg, 2.0 mmol), and the resulting mixture was stirred for 12 h at 60 °C. The final yellow solution was concentrated to ca. 1 mL and pentane (6 mL) was added, causing the precipitation of a whitish solid. The precipitate was decanted, washed with pentane (4 × 8 mL), and dried in vacuo. An ivory solid was obtained. Yield: 702 mg (70%). Anal. Calcd for $C_{16}H_{41}ClN_3OsP$: C, 36.11; H, 7.77; N, 7.90. Found: C, 35.74; H, 7.40; N, 7.82. IR (cm^{-1}): 3114 (s, NH), 2117 (s, OsH), 2078 (m, OsH). $^{31}P\{^1H\}$ NMR (CD_3CN , 298 K): δ 29.7 (s). 1H NMR (CD_3CN , 298 K): δ -12.06 (d, $^2J_{HP} = 15.9$ Hz, 3 H, Os–H), 1.14 (dd, $^3J_{HP} = 12.6$ Hz, $^3J_{HH} = 7.2$ Hz, 18 H, PCHCH₃), 1.96 (m, 3 H, PCHCH₃), 1.70–3.50 (14 H, -CH₂-), 5.43 (br, 2 H, NH), 5.69 (br, 1 H, NH). $T_{1(\min)}$ (ms, OsH, CD_2Cl_2 , 213 K): 75 ± 1 .

Preparation of $[OsH_2(TACD)(\eta^2-H_2)(P^iPr_3)](BF_4)_2$ (5). HBF₄ (1:1 solution in diethyl ether, 300 μ L, 2.2 mmol) was added to a dichloromethane (10 mL) suspension of **4** (318 mg, 0.60 mmol), and the mixture was stirred for 10 min. The resulting suspension was concentrated to ca. 3 mL, and diethyl ether (15 mL) was added. The solid was decanted, washed with diethyl ether (3 × 15 mL), and dried in vacuo. A white solid was obtained. Yield: 329 mg (82%). Anal. Calcd for $C_{16}H_{42}B_2F_8N_3OsP$: C, 28.63; H, 6.31; N, 6.26. Found: C, 28.70; H, 6.15; N, 6.30. IR (cm^{-1}): 3282 (m, NH), 1006 (vs, BF_4^-). $^{31}P\{^1H\}$ NMR (CD_3CN , 298 K): δ 51.3 (s). 1H NMR (CD_3CN , 298 K): δ -9.11 (d, $^2J_{HP} = 19.8$ Hz, 4 H, Os–H), 1.27 (dd, $^3J_{HP} = 16.2$ Hz, $^3J_{HH} = 7.2$ Hz, 18 H, PCHCH₃), 2.40 (m, 3 H, PCHCH₃), 1.80–3.80 (14 H, -CH₂-), 6.16 (br, 2 H, NH), 6.40 (br, 1 H, NH). $T_{1(\min)}$ (ms, OsH, $CDCl_2F/CD_3CN$ (2:1), 218 K): 23 ± 1 .

Preparation of $[OsH_3(BAEA)(P^iPr_3)Cl]$ (6). To a brown toluene solution (20 mL) of **1**, generated in situ from $OsH_2Cl_2(P^iPr_3)_2$ (750 mg, 1.28 mmol), molecular hydrogen, and triethylamine, was added BAEA (180 mg, 1.67 mmol), and the resulting mixture was stirred for 12 h at 60 °C. The resulting ivory suspension was vacuum-dried, and the residue was washed with diethyl ether (4 × 6 mL) and dried in vacuo. A white solid was obtained. Yield: 75 mg (62%). Anal. Calcd for $C_{13}H_{37}ClN_3OsP$: C, 31.73; H, 7.58; N, 8.54. Found: C, 31.90; H, 7.75; N, 8.83. IR (cm^{-1}): 3228, 3139 (m, NH), 2136, 2106 (m, Os–H). $^{31}P\{^1H\}$ NMR (CD_3CN , 298 K): δ 39.0 (s). 1H NMR (CD_3CN , 298 K): δ -12.38 (d, $^2J_{HP} = 14.7$ Hz, 3 H, Os–H), 1.11 (dd, 18 H, $^3J_{HP} = 12.3$ Hz, $^3J_{HH} = 6.9$ Hz, PCHCH₃), 1.92 (m, 6 H, PCHCH₃), 2.60–3.20 (12 H, -CH₂-N); 4.17, 5.17, 5.63 (all br, 5H, NH). $T_{1(\min)}$ (ms, OsH, CD_2Cl_2 , 203 K): 77 ± 1 .

Preparation of $[Os(BAEA)(\eta^2-H_2)_2(P^iPr_3)](BF_4)_2$ (7). HBF₄ (1:1 solution in diethyl ether, 200 μ L, 1.47 mmol) was added to a solution of **6** (256 mg, 0.52 mmol) in dichloromethane (15 mL). After 10 min of stirring, the mixture was concentrated to ca. 3 mL and diethyl ether (10 mL) was added. The resulting solid was decanted, washed with cold diethyl ether (-60 °C, 3 × 10 mL), and dried in vacuo. A whitish solid was obtained. Yield: 295 mg (90%). Anal. Calcd for $C_{13}H_{38}B_2F_8N_3OsP$: C, 24.73; H, 6.07; N, 6.66. Found: C, 24.90; H, 6.10; N, 7.01. IR

(cm^{-1}): 3329, 3281 (m, NH), 2041 (vw, OsH₂), 1024 (vs, BF_4^-). $^{31}P\{^1H\}$ NMR (CD_3CN , 298 K): δ 32.5 (s). 1H NMR (CD_3CN , 298 K): δ -10.31 (d, $^2J_{HP} = 8.1$ Hz, 4 H, Os–H), 1.22 (dd, 18 H, $^3J_{HP} = 14.4$ Hz, $^3J_{HH} = 6.6$ Hz, PCHCH₃), 2.46 (m, 3 H, PCHCH₃), 2.80–3.20 (all m, 12 H, -CH₂-N), 4.09 (br, 1H, NH), 4.82, 6.79 (both br, 2H each, NH₂). $T_{1(\min)}$ (ms, OsH, $CDCl_2F/CD_3CN$ (2:1), 218 K): 14 ± 1 .

Structural Analysis of Complexes 2–4 and 6. Crystals suitable for the X-ray diffraction study were obtained at room temperature by vapor diffusion of diethyl ether into solutions of the complexes in acetonitrile or dichloromethane. X-ray data were collected for all complexes on a Bruker Smart APEX CCD diffractometer equipped with a normal-focus, 2.4 kW sealed tube source (Mo radiation, $\lambda = 0.71073$ Å) operating at 50 kV and 40 mA (**2** and **3**) or 30 mA (**4** and **6**). Data were collected over the complete sphere by a combination of four sets. Each frame exposure time was 20 s (**2** and **3**) or 10 s (**4** and **6**), covering 0.3° in ω . Data were corrected for absorption by using a multiscan method applied with the SADABS program.³⁶ The structures of all compounds were solved by the Patterson method. Refinement, by full-matrix least squares on F^2 with SHELXL97,³⁷ was similar for all complexes, including isotropic and subsequently anisotropic displacement parameters. The hydrogen atoms bonded to the metal center were observed in the difference Fourier maps and refined with a restrained Os–H bond length of 1.59(1) Å (CSD). The rest of the hydrogen atoms were observed or calculated and refined freely or using a restricted riding model. For complex **3**, one of the two BF_4^- anions was observed disordered. The anion was defined with two moieties, complementary occupancy factors, isotropic atoms, and restrained geometry. In all complexes, all of the highest electronic residuals were observed in close proximity to the osmium centers and make no chemical sense.

Crystal data for **2**: $C_{15}H_{39}ClN_3OsP$, $M_w = 518.11$, colorless, plate (0.12 × 0.10 × 0.02), monoclinic, space group $C2/c$, $a = 35.985(6)$ Å, $b = 8.0796(14)$ Å, $c = 14.499(3)$ Å, $\beta = 99.758(3)^\circ$, $V = 4154.5(12)$ Å³, $Z = 8$, $D_{\text{calc}} = 1.657$ g cm^{-3} , $F(000) = 2064$, $T = 100(2)$ K, $\mu = 6.344$ mm⁻¹, 25 260 measured reflections ($2\theta = 3$ –58°, ω scans 0.3°), 5144 unique ($R_{\text{int}} = 0.0418$); min/max transmission factors 0.397/0.691. Final agreement factors were $R1 = 0.0312$ [4195 observed reflections, $I > 2\sigma(I)$] and $wR2 = 0.0652$; data/restraints/parameters 5144/4/218; GOF = 0.955. Largest peak and hole = 2.250 and -2.067 e/Å³.

Crystal data for **3**: $C_{15}H_{40}B_2F_8N_3OsP \cdot CH_3CN$, $M_w = 698.34$, colorless, irregular block (0.18 × 0.10 × 0.09), monoclinic, space group $P2(1)/n$, $a = 8.1936(14)$ Å, $b = 33.085(6)$ Å, $c = 9.7024(16)$ Å, $\beta = 94.868(3)^\circ$, $V = 2620.7(8)$ Å³, $Z = 4$, $D_{\text{calc}} = 1.770$ g cm^{-3} , $F(000) = 1384$, $T = 100(2)$ K, $\mu = 4.997$ mm⁻¹, 17 705 measured reflections ($2\theta = 3$ –58°, ω scans 0.3°), 6245 unique ($R_{\text{int}} = 0.0572$); min/max transmission factors 0.455/0.639. Final agreement factors were $R1 = 0.0410$ [5011 observed reflections, $I > 2\sigma(I)$] and $wR2 = 0.0829$; data/restraints/parameters 6245/25/330; GOF = 0.988. Largest peak and hole = 2.096 and -1.379 e/Å³.

Crystal data for **4**: $C_{16}H_{41}ClN_3OsP$, $M_w = 532.14$, colorless, irregular block (0.12 × 0.06 × 0.06), monoclinic, space group $P2(1)/n$, $a = 11.0652(12)$ Å, $b = 13.6318(15)$ Å, $c = 14.0989(15)$ Å, $\beta = 101.078(2)^\circ$, $V = 2087.0(4)$ Å³, $Z = 4$, $D_{\text{calc}} = 1.694$ g cm^{-3} , $F(000) = 1064$, $T = 100(2)$ K, $\mu = 6.316$ mm⁻¹, 18 532 measured reflections ($2\theta = 3$ –58°, ω scans 0.3°), 5114 unique ($R_{\text{int}} =$

(36) Blessing, R. H. *Acta Crystallogr.* **1995**, *A51*, 33. SADABS: Area-detector absorption correction; Bruker-AXS: Madison, WI, 1996.

(37) SHELXTL Package, version 6.10; Bruker-AXS: Madison, WI, 2000. Sheldrick, G. M. *Acta Crystallogr.* **2008**, *A64*, 112.

0.0411); min/max transmission factors 0.475/0.682. Final agreement factors were $R1 = 0.0284$ [4418 observed reflections, $I > 2\sigma(I)$] and $wR2 = 0.0567$; data/restraints/parameters 4418/0/215; GOF = 1.042. Largest peak and hole = 1.139 and $-1.101 e/\text{\AA}^3$.

Crystal data for **6**: $C_{13}H_{37}ClN_3OsP \cdot CH_2Cl_2$, $M_w = 577.00$, colorless, irregular block ($0.12 \times 0.12 \times 0.06$), monoclinic, space group $P2_1$, $a = 8.3616(6) \text{\AA}$, $b = 9.5846(7) \text{\AA}$, $c = 13.6773(11) \text{\AA}$, $\beta = 91.9300(10)^\circ$, $V = 1095.51(14) \text{\AA}^3$, $Z = 2$, $D_{\text{calc}} = 1.749 \text{ g cm}^{-3}$, $F(000) = 572$, $T = 100(2) \text{ K}$, $\mu = 6.260 \text{ mm}^{-1}$, 13 759 measured reflections ($2\theta = 3\text{--}58^\circ$, ω scans 0.3°), 5277 unique ($R_{\text{int}} = 0.0243$); min/max transmission factors 0.518/0.682. Final agreement factors were $R1 = 0.0199$ [5191 observed reflections, $I > 2\sigma(I)$] and $wR2 = 0.0440$; data/restraints/parameters 5277/4/215; GOF = 0.987. Largest peak and hole = 0.898 and $-0.874 e/\text{\AA}^3$.

Computational Details. Quantum mechanical calculations were performed with the *Gaussian03* package³⁸ at the DFT B3PW91 level.^{39,40} Core electrons of the osmium atom were described using the effective core pseudopotentials of Hay–Wadt, and valence electrons were described with the standard LANL2DZ basis set.⁴¹ A set of f-type functions was also added.⁴² Carbon atoms were

described with a 6-31G basis set.⁴³ The hydrogen atoms directly bonded to the osmium and nitrogen centers were described with a 6-31G(d,p) set of basis functions.⁴³ The rest of the hydrogen atoms were described with a 6-31G basis set.⁴³ All minima were characterized by analytically computing the Hessian matrix. Information on the atom coordinates (xyz files) for all optimized structures is collected in the Supporting Information.

Acknowledgment. Financial support from the MICINN of Spain (Projects CTQ2008-00810 and Consolider Ingenio 2010 CSD2007-00006) and Diputación General de Aragón (E35) is acknowledged. M.B. thanks the Spanish MICINN/Universidad de Zaragoza for funding through the “Ramón y Cajal” program.

Supporting Information Available: X-ray analysis and crystal structure determinations, including bond lengths and angles of compounds **2–4** and **6**, the full list of authors for ref 38, and orthogonal coordinates and absolute energies of the optimized theoretical structures. This material is available free of charge via the Internet at <http://pubs.acs.org>.

IC8023259

- (38) Frisch, M. J.; et al. *Gaussian 03*, revision C.02; Gaussian, Inc.: Wallingford, CT, 2004 (for the complete reference, see the Supporting Information).
- (39) Becke, A. D. *J. Chem. Phys.* **1993**, *98*, 5648.
- (40) (a) Perdew, J. P. In *Electronic Structure of Solids*, 91st ed.; Ziesche, P.; Eschrig, H., Eds.; Akademie Verlag: Berlin, 1991; p 11. (b) Perdew, J. P.; Wang, Y. *Phys. Rev. B* **1992**, *45*, 13244. (c) Perdew, J. P.; Burke, K.; Wang, Y. *Phys. Rev. B* **1996**, *54*, 16533.
- (41) Hay, P. J.; Wadt, W. R. *J. Chem. Phys.* **1985**, *82*, 270.
- (42) Ehlers, A. W.; Böhme, M.; Dapprich, S.; Gobbi, A.; Höllwarth, A.; Jonas, V.; Kohler, K. F.; Stegmann, R.; Veldkamp, A.; Frenking, G. *Chem. Phys. Lett.* **1993**, *208*, 111.

- (43) (a) Ditchfield, R.; Hehre, W. J.; Pople, J. A. *J. Chem. Phys.* **1971**, *54*, 724. (b) Hehre, W. J.; Ditchfield, R.; Pople, J. A. *J. Chem. Phys.* **1972**, *56*, 2257. (c) Hariharan, P. C.; Pople, J. A. *Mol. Phys.* **1974**, *27*, 209. (d) Gordon, M. S. *Chem. Phys. Lett.* **1980**, *76*, 163. (e) Hariharan, P. C.; Pople, J. A. *Theor. Chim. Acta* **1973**, *28*, 213. (f) Blaudeau, J.-P.; McGrath, M. P.; Curtiss, L. A.; Radom, L. *J. Chem. Phys.* **1997**, *107*, 5016. (g) Francl, M. M.; Pietro, W. J.; Hehre, W. J.; Binkley, J. S.; DeFrees, D. J.; Pople, J. A.; Gordon, M. S. *J. Chem. Phys.* **1982**, *77*, 3654. (h) Binning, R. C., Jr.; Curtiss, L. A. *J. Comput. Chem.* **1990**, *11*, 1206. (i) Rassolov, V. A.; Pople, J. A.; Ratner, M. A.; Windus, T. L. *J. Chem. Phys.* **1998**, *109*, 1223. (j) Rassolov, V. A.; Ratner, M. A.; Pople, J. A.; Redfern, P. C.; Curtiss, L. A. *J. Comput. Chem.* **2001**, *22*, 976.